

**ARTICLE TYPE****MIMO Antenna Selection Using Biogeography Based Optimization with Non-Linear Migration Models**Konstantinos C. Fountoukidis<sup>1</sup> | Christos Kalialakis<sup>2</sup> | Kostas E. Psannis<sup>3</sup> | Katherine Siakavara<sup>1</sup> | Sotirios K. Goudos<sup>1</sup> | Panagiotis Sarigiannidis\*<sup>4</sup> | Mohammad Obaidat<sup>5</sup><sup>1</sup>Department of Physics, Aristotle University of Thessaloniki, Thessaloniki 54124, Greece<sup>2</sup>Microwave Systems and Nanotechnology Department, CTTC, Castelldefels, Spain<sup>3</sup>Department of Applied Informatics, School of Information Sciences, University of Macedonia, Thessaloniki, Greece<sup>4</sup>Department of Informatics and Telecommunications Engineering, University of Western Macedonia, Karamanli & Ligeris, Kozani, 50100, Greece<sup>5</sup>King Abdullah II School of IT, University of Jordan, x, Jordan**Correspondence**

\*Panagiotis Sarigiannidis, Department of Informatics and Telecommunications Engineering, University of Western Macedonia, Karamanli &amp; Ligeris, Kozani, 50100, Greece Email: psarigiannidis@uowm.gr

**Summary**

This paper deals with the problem of antenna selection (AS) for a multiple-input multiple-output (MIMO) wireless system under the constraint of the channel capacity maximization. The biogeography-based optimization (BBO) algorithm is applied on the joint transmitter and receiver AS problem. Moreover, the performance of different BBO migration models is compared with a real valued genetic algorithm (RVGA) as well as with the ant colony optimization (ACO). Representative simulation scenarios are provided in detail, involving selection of  $2 \times 4$ ,  $3 \times 5$ ,  $4 \times 6$ ,  $8 \times 8$  antennas in a  $16 \times 16$  MIMO system. The numerical results demonstrate the efficiency and the applicability of the BBO algorithm in modern MIMO wireless systems.

**KEYWORDS:**

ant colony optimization; antenna selection; biogeography-based optimization; evolutionary algorithms; genetic algorithm; multiple-input multiple-output systems

**1 | INTRODUCTION**

Nowadays, there is a growing need for higher data rates, which makes MIMO antenna systems important to a greater extent. MIMO wireless broadcast systems can achieve high data rates through spatial multiplexing gain and improved reliability via diversity gain<sup>1,2,3</sup>. However, when multiple antennas at the transmitter and the receiver side of any connection are used, this results to an increase of hardware complexity and cost considering the analog radio frequency (RF) chains (i.e., amplifiers, analog to digital (A/D) converters and filters) per antenna. The authors in<sup>4</sup> have showed that one way to reduce costs for hardware will be to choose a proper subset of antennas from the set of the all antennas and then use only these selected antennas. In this way, the advantage of MIMO is maintained and the complexity is mitigated.

The antenna selection (AS) method becomes even more important within the emerging massive MIMO technology<sup>5,6,7,8</sup>. Thus, it is desirable to have a larger antenna number than the RF chains number in each link end and to choose the antenna subset that will be in use. However, the reduction of the antenna number will certainly cause performance deterioration. For this reason,

<sup>0</sup>**Abbreviations:** AS, antenna selection; MIMO, multiple-input multiple-output; BBO, biogeography-based optimization; RF, radio frequency; A/D, analog to digital; ES, exhaustive search; DTRS, decoupled transmit-receive selection; STRSS, separable transmit-receive successive selection; SJTRS, successive joint transmit-receive selection; EJTRAS, efficient joint transmit-receive antenna selection; GA, genetic algorithm; BPSO binary particle swarm optimization; SGA, GA-based algorithm; PGA, priority GA; RVGA real-valued genetic algorithm; CSI, channel state information; GAS, genetic antenna selection; CEE, channel estimation error; HSI, habitat suitability index; CCDF, complimentary cumulative distribution function

the selection of an optimal algorithm that will give good results is very important. This question translates to which antenna subset should be chosen from each link end in order to provide the maximum channel capacity. In other words, the principle of AS is to choose the best  $L_R$  out of  $K_R$  antennas located at the receiver side and the best  $L_T$  out of  $K_T$  antennas located at the transmitter side. Therefore, the AS problem is a combinatorial optimization problem where all the problem decision variables are in binary space.

An exhaustive search (ES) approach for solving this problem is to search over all possible combinations of antennas in each side (ES). However, this method will result in undesired computational complexity. Hence, the only way to counterbalance this high computational complexity is to find sub-optimal algorithms with performance as close as possible to the one provided by the ES.

Several approaches have appeared in the literature that address the antenna selection problem<sup>9,10,11,12,13,14,15,16</sup>. There is a considerable amount of studies available in the literature aiming to fulfill the antenna selection criterion, that propose different sub-optimal algorithms, for channel capacity maximization. A separable transmit-receive successive selection (STRSS) as well as a successive joint transmit-receive selection (SJTRS) were proposed and compared in terms of spectral efficiency and outage probability. Later, a computationally efficient joint transmit-receive antenna selection (EJTRAS) algorithm was presented in<sup>9</sup>, having improved performance compared to the previous decoupling methods.

Apart from decoupling-based algorithms mentioned in the previous paragraph, evolutionary algorithms were applied in the same problem. These approaches include genetic algorithms (GAs)<sup>17,18,19,20</sup>, and binary particle swarm optimization (BPSO)<sup>21,22,23</sup>. However, in most of these approaches the algorithms work in real space and map the real values to binary space. In this paper, we apply algorithms that are better suited to work in binary spaces and combinatorial optimization problems. Biogeography-based optimization (BBO)<sup>24</sup> is an evolutionary algorithm, which is derived from a specific field in Biology, the biogeography. BBO uses formulas that model the migration patterns of different animals between islands. BBO solves an optimization problem through an iterative procedure using migration and mutation operators. The original BBO uses a linear model for the migration operator. However, in order to improve BBO performance, authors in<sup>25</sup> introduce two new nonlinear migration models, namely model 7 and model 8. Several papers exist in the literature that apply BBO to antenna design problems. Among others, these papers include Yagi-Uda antenna synthesis<sup>26</sup>, microstrip antenna design<sup>27,28</sup> and antenna array synthesis<sup>29,30,31,32</sup>.

The goal of this paper is to apply BBO with different migration models to a joint transmit-receive antenna selection problem. In particular, we extend and advance of our earlier work<sup>33</sup>. To the best of our knowledge, this is the first time that the BBO algorithm with non-linear migration models is used for solving the AS problem. This paper contributes also to the performance comparison of several EAs to different AS problem cases. Additionally, this work offers design cases which could be also used as a framework of benchmark functions for testing evolutionary algorithms to complex combinatorial optimization problems. To this end, we evaluate the BBO algorithms performance with other popular metaheuristics. These are the ant colony optimization (ACO)<sup>34,35</sup>, which is a swarm intelligence algorithm that models the ants' foraging behavior. The authors in<sup>36,37</sup> have successfully used ACO for thinned array design. The second method used for comparison is the real-valued genetic algorithm (RVGA) introduced in<sup>18</sup>.

The rest of this paper is organized as follows. **Section 2 presents the related work**. The antenna selection problem formulation is described in Section 3. A brief description of the BBO algorithm used in this paper is given in Section 4. In Section 5, numerical results for four antenna selection cases in a  $16 \times 16$  MIMO system are presented and compared by suitable statistical tests. Finally, conclusions are drawn in Section 6.

## 2 | RELATED WORK

There are several papers in the literature addressing the AS problem. In<sup>11</sup> the authors consider antenna subset selection employing space-time coding, taking two cases assuming different type of channel knowledge. The problem of only receive antenna selection is examined by the authors in<sup>12</sup> by introducing new selection algorithms for maximizing the channel capacity. A review paper that discusses the AS problem algorithms is given in<sup>13</sup>. Moreover, the authors in<sup>14</sup> introduce a generic methodology that can be used not only in AS problems but also for any MIMO system where partial CSI is available at the transmitter side. A new algorithm that solves the AS problem on the receive side and is based on the minimization of the union bound on the vector error rate is proposed in<sup>16</sup>. The authors relax the AS problem variables from discrete to continuous and thus solve it using convex optimization. Additionally, in<sup>10</sup> the authors present a antenna selection protocol designed for IEEE 802.16/WiMax stations, the protocol performance is verified by OPNET simulations.

The authors in<sup>15</sup> obtain measurement data from a MIMO antenna and study the transmitting antenna selection from four elements to two elements. In<sup>9</sup> the authors propose a joint transmit and receive AS (EJTRAS) algorithm. The new algorithm according to the authors may produce near optimal outage and ergodic capacity results with low complexity.

The use of evolutionary methods for solving the AS problem is introduced in<sup>17</sup>. The authors in<sup>17</sup> proposed a simple GA-based algorithm (SGA) resulting in reduced hardware complexity. In<sup>19</sup>, a priority GA (PGA) was presented achieving superior performance compared to SGA in terms of capacity and computational complexity. The main difference between SGA and PGA lies to the fact that the later one consists of chromosomes with integer string while the former one uses a bit string. The authors in<sup>20</sup> propose a joint symbol detection and receive antenna selection framework, which uses the maximum likelihood (ML) criterion. They apply a new GA variant, the heterogeneous GA (HGA), where the chromosome has two strings, one discrete (integer) that represents the antenna selection and one bit string that represents the symbol detection. Moreover, the real-valued genetic algorithm (RVGA) was introduced in<sup>18</sup>, where its chromosomes are random priority magnitude vectors. It has been shown that, RVGA outperforms all the aforementioned sub-optimal AS algorithms in different antenna sub-set scenarios. More recently, a genetic antenna selection (GAS) algorithm was introduced in<sup>38</sup> for Massive MIMO systems given the channel estimation error (CEE) at the receiver side.

The authors in<sup>21</sup> use a Binary Particle Swarm Optimization variant (BPSO) for solving the AS problem. The authors improve the original BPSO by tailoring it specifically for the AS problem and they increase convergence speed. The same authors in<sup>22</sup> extend the AS problem by solving the real-time joint user scheduling and receive antenna selection (JUSRAS) in multiuser MIMO systems. Additionally, they also apply the same BPSO algorithm. Binary PSO is also applied in<sup>23</sup> for a cross layer antenna selection optimization problem. More specifically, the authors truncated selective repeat automatic repeat request (TSR-ARQ) at data link layer, for increasing the MIMO system throughput, thus the throughput of the data-link layer is the fitness value of the BPSO algorithm.

The BBO algorithm was introduced in<sup>24</sup>. Since then there has been a growing research interest in producing improved modifications of the original algorithm and in applying the BBO and its variants to real-world engineering problems. The original algorithm uses a linear migration model. The author in<sup>39</sup> studies the performance of six different migration models using test functions. The author concludes that sinusoidal migration curves obtained the best performance. Moreover, the authors in<sup>25</sup> complete the previous works by mathematically analyzing the BBO migration model. This mathematical analysis helps them to introduce two new non-linear models, namely model 7 (BBO7) and model 8 (BBO8). The authors perform several simulations on benchmark functions and compare different BBO migration models as well as other EAs.

Moreover, the application of the original BBO algorithm to Yagi-Uda antenna design is investigated by the authors in<sup>26</sup>. The authors in<sup>27</sup> present a modified BBO (MBBO) algorithm, which is used for designing circular microstrip antennas. Additionally, the authors in<sup>28</sup> design rectangular microstrip antennas with the original BBO algorithm. Linear and circular array design using the original BBO algorithm is presented in<sup>31</sup>. Additionally, the authors in<sup>32</sup> use BBO for obtaining the suitable antenna amplitudes in a linear antenna array. The application of the original BBO to antenna array design with a reduced number of elements is reported in<sup>29</sup>. Furthermore, in<sup>30</sup> the authors use the original BBO as well as BBO with other migration models in order to design large antenna thinned array design.

### 3 | MIMO SYSTEM MODEL

We consider MIMO system that uses spatial multiplexing in a frequency non-selective fading wireless channel. This MIMO system has  $K_T$  antennas for transmission and  $K_R$  antennas for reception. Then, the complex  $K_R \times 1$  signal vector  $\mathbf{y}$  can be expressed with the following form:

$$\mathbf{y} = \sqrt{\frac{E_x}{N_T}} \mathbf{H} \mathbf{x} + \mathbf{z} \quad (1)$$

where  $\mathbf{x} = [x_1, x_2, \dots, x_{K_T}]^T$  is the complex  $K_T \times 1$  transmitted symbol vector,  $E_x$  is the constant signal energy of each transmitted signal  $x_i$ , which is transmitted from the  $i$ -th transmit antenna. Additionally,  $\mathbf{H}$  is the  $K_R \times K_T$  channel matrix, where the element  $h_{km}$  stands for the link gain from between the  $k$ -th transmit antenna to the  $m$ -th receive antenna. This link gain is assumed to be a zero-mean and unit variance (i.i.d) complex Gaussian random variable. Moreover,  $\mathbf{z} = [z_1, z_2, \dots, z_{K_R}]^T$  represents the  $K_R \times 1$  white complex Gaussian noise vector with zero-mean and covariance matrix  $N_0 I_{K_R}$ , where  $I_{K_R}$  is a  $K_R \times K_R$  identity matrix.

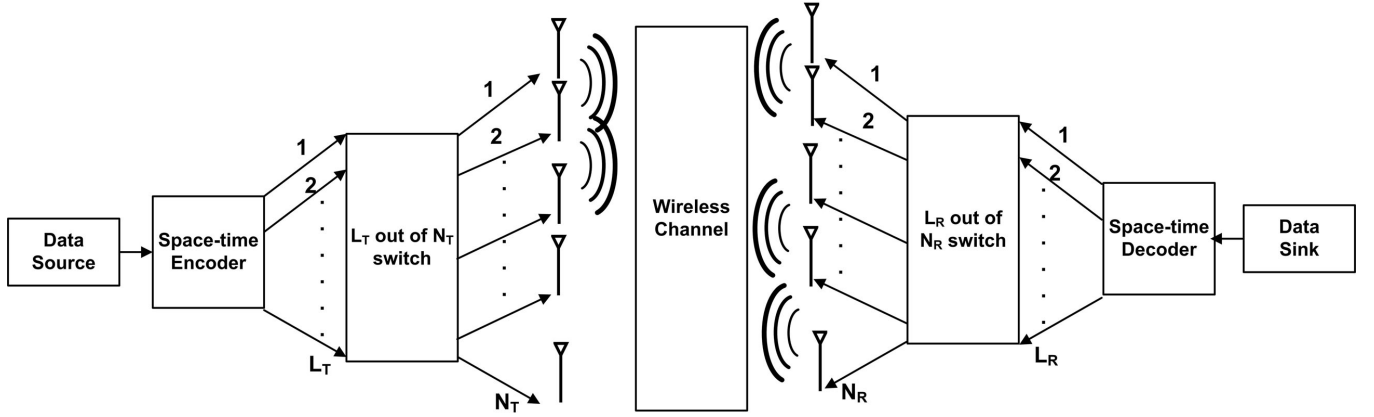


FIGURE 1 A typical MIMO system model which includes antenna selection.

We make the following assumptions: the CSI is available at the receive side only and the transmitted complex vector  $\mathbf{x}$  is statistically independent, i.e.,  $E\{xx^H\} = \mathbf{I}_{K_T}$ , where  $E\{\cdot\}$  is the expected value operator. Thus, the capacity of the deterministic MIMO channel can be represented by<sup>4,2</sup>:

$$C = \log_2 \det \left( \mathbf{I}_{N_T} + \frac{E_x}{K_T N_0} \mathbf{H}^H \mathbf{H} \right) \quad (2)$$

where  $\det(\cdot)$  and  $(\cdot)^H$  are the determinant and the Hermitian operator, respectively. Equation (2) is applicable when  $K_R \geq K_T$ <sup>3</sup>.

Figure 1 presents a typical topology for a MIMO system. Suppose that there are  $L_T$  and  $L_R$  RF chains at the transmit and receive sides respectively,  $L_T \leq K_T$  and  $L_R \leq K_R$ . Thus, the primary objective in the antenna selection problem is to select the optimal antenna subset. That is to select  $L_T$  out of  $K_T$  antennas at the transmitter side and  $L_R$  out of  $K_R$  antennas at the receiver side, in order to maximize the capacity expressed by<sup>4</sup>:

$$\bar{C} = \log_2 \det \left( \mathbf{I}_{L_T} + \frac{E_x}{L_T N_0} \bar{\mathbf{H}}^H \bar{\mathbf{H}} \right) \quad (3)$$

where  $\bar{\mathbf{H}}$  denotes a  $L_R \times L_T$  sub-block matrix of  $\mathbf{H}$ . Taking into account that, for a MIMO wireless system with  $K_T \times K_R$  antennas there will be  $K_{select}$  different possibilities of selection of  $(L_R, L_T)$  antennas in operation given by:

$$K_{select} = C_{K_T, L_T} \times C_{K_R, L_R} = \binom{K_T}{L_T} \times \binom{K_R}{L_R} \quad (4)$$

The AS optimization problem is therefore expressed by:

$$\max_{\mathbf{b}} \bar{C}(\mathbf{b}) = \log_2 \det \left( \mathbf{I}_{L_T} + \frac{E_x}{L_T N_0} \bar{\mathbf{H}}^H(\mathbf{b}) \bar{\mathbf{H}}(\mathbf{b}) \right) \quad (5)$$

where  $\mathbf{b} = [b_1, b_2, \dots, b_{K_R}, b_{N_{R+1}}, \dots, b_{K_R+K_T}]$  is a  $K_T + K_R$  binary vector. If  $b_i = 1$  then the antenna in position  $i$  is selected to transmit or receive depending on the position, otherwise the antenna does not operate. In case of a large antenna number like in Massive MIMO, using the ES method is a compute-intensive application and thus not practical.

## 4 | THE ANTENNA SELECTION ALGORITHMS

### 4.1 | The ACO algorithm

Ant colony optimization (ACO)<sup>34,35</sup> is a global optimization algorithm that is based on ants' behavior. The ants communicate with each other using chemical pheromone trails. By following these trails the ants can find short paths between their nest and possible food sources. Thus, the ants sensing of pheromone is done the following way. The ants select to follow trails with strong

pheromone intensities. That way they tend to follow the shorter paths than the longer ones. ACO algorithm models this type of behavior and is widely used for solving combinatorial optimization problems.

## 4.2 | The RVGA algorithm

The RVGA introduced in<sup>18</sup> is a real-valued genetic algorithm that uses the operators of mutation, crossover and selection. In RVGA each chromosome is a real number. Two random chromosomes are selected from the current population based on a selection strategy. Then, crossover is applied to get features from both original parents to produce a child chromosome. The crossover operator application depends on predetermined crossover probability. In a similar way, the new generated child may mutate based on a predefined mutation probability.

## 4.3 | The BBO algorithm

BBO<sup>24</sup> uses the mathematical models of Biogeography for predicting animal migration patterns. These patterns help in estimating the number of species in a habitat. In BBO terminology, a geographically isolated area is called a habitat. BBO maps a habitat suitability index (HSI) value to each habitat. BBO models these features as suitability index variables (*SIV*). The *SIV*s are the unknowns in a optimization problem, while *HSI* is objective function value. Therefore, we can model in BBO each potential solution to the antenna selection as a binary string of *SIV* variables. For the case of the antenna selection problem, the number of dimensions becomes  $K_T + K_R$  and the vector of the unknown variables is  $\mathbf{h} = [SIV_1, SIV_2, \dots, SIV_{K_R}, SIV_{K_R+1}, \dots, SIV_{K_R+K_T}]$ . In the antenna selection problem, vector  $\mathbf{h}$  denotes the priority magnitude vector (*PMV*), which is related with  $K_R$  receive and  $K_T$  transmit antennas. A binary string is used to model each habitat. The *SIV*s that have a binary value of one represent the higher priority for selection of the corresponding antenna element. Therefore,  $\bar{\mathbf{H}}$  contains the rows with the  $L_R$  larger values out of the first  $K_R$  elements in *PMV*. Moreover,  $\bar{\mathbf{H}}$  contains the columns of the  $L_T$  larger values out of the last  $K_T$  elements in *PMV*.

The *HSI* value of a habitat or vector is the objective function value. Therefore, vectors that have high *HSI* values represent the solutions with high channel capacity value. The emigration rate  $\psi$  of these solutions is high because they have a large number of species, while the immigration rate  $\xi$  is low. On the other hand, the bad solution vectors have low *HSI* value (low channel capacity). Thus, this means that they have low emigration  $\psi$  and high immigration  $\xi$  rates, respectively.

The immigration rate  $\xi$  and emigration rate  $\psi$ , for the linear model, are expressed by<sup>24</sup>:

$$\psi_k = E \left( \frac{k}{Q_{\max}} \right) \quad (6)$$

$$\xi_k = I \left( 1 - \frac{k}{Q_{\max}} \right) \quad (7)$$

where  $E$  is the maximum possible emigration rate,  $k$  is the species number of the  $k$ -th habitat,  $Q_{\max}$  is the maximum number of species and  $I$  is the maximum possible immigration rate. The immigration rate  $\xi$  and emigration rate  $\psi$  are linear functions of the number of species  $k$  in the habitat, as it can be seen from the equations 6 and 7. Figure 2 depicts this relationship in a graphic manner. Thus, if the the number of species in a habitat increases then the immigration rate linearly decreases, while the emigration rate linearly increases. This means that when the more crowded the habitat becomes the fewer species can be successful immigrants to that habitat. On the other hand, in this case more species are more probable to leave the habitat to other habitats. However, as it reported in<sup>39</sup>, the linear models are a simple approximation of complicated phenomena in Nature like migration. This fact creates the need for nonlinear migration models in order to model more accurately the migration phenomenon. The authors in<sup>25</sup> propose two new non-linear migration models. They have conducted a theoretical analysis of BBO where they

define the quantity  $K = \frac{\sum_{n=1}^{NP} \sum_{m=1}^n \psi_m}{NP}$ . According to them, a BBO algorithm with large  $K$  may perform better. Therefore, they have

designed the new non-linear models based on the above principle. It must be noted that immigration rate  $\xi$  is the same in both models and is a sinusoidal functions of the number of species  $k$ , thus obtaining resulting in a bell-like shape. This type of model describes better the natural phenomena in a habitat. The emigration rate  $\psi$  is different in both models and it a convex function of the number of species  $k$ . For the non-linear models, called model 7 (BBO7) and model 8 (BBO8), the emigration rate  $\psi$  and the immigration rate  $\xi$  are described by<sup>25</sup>:

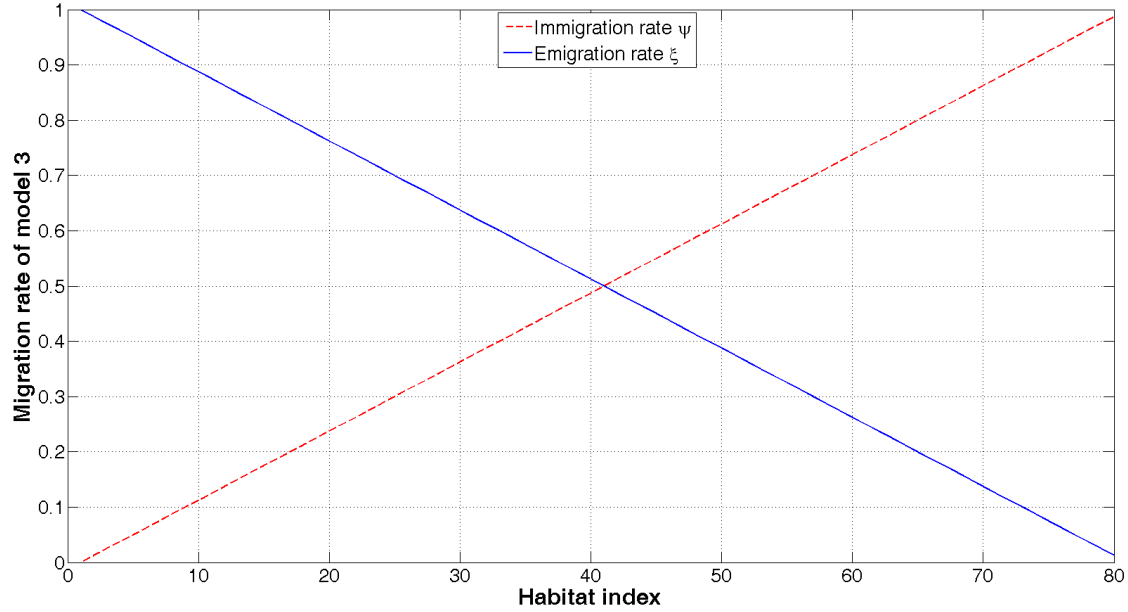


FIGURE 2 Migration Model 3: Habitat index vs migration rates for population size  $NP = 80$

1) Model 7

$$\psi_k = E\left(\frac{k}{Q_{\max}}\right)^4, \quad \xi_k = \frac{I}{2} \left( \cos\left(\frac{k\pi}{Q_{\max}}\right) + 1 \right) \quad (8)$$

2) Model 8

$$\psi_k = E\left(\frac{k}{Q_{\max}}\right)^{16}, \quad \xi_k = \frac{I}{2} \left( \cos\left(\frac{k\pi}{Q_{\max}}\right) + 1 \right) \quad (9)$$

Figures 3-4 depict graphically the relationship between habitat index and migration rates for models 7 and 8 respectively. The migration for  $NP$   $PMV$ s can be described as follows in Algorithm 1.

---

**Algorithm 1**  $PMV$  migration

---

```

1: for  $n=1$  to  $NP$  do
2:   Choose  $PMV_n$  using probability that depends on  $\xi_n$ 
3:   if  $random(0, 1) < \xi_n$  then
4:     for  $m=1$  to  $NP$  do
5:       Choose  $PMV_m$  using probability that depends on  $\psi_m$ 
6:       if  $random(0, 1) < \psi_m$  then
7:         Choose a  $SIV$   $\sigma$  from  $X_m$  randomly
8:         Choose a  $SIV$  in  $PMV_n$  randomly to replace it with  $\sigma$ 
9:       end if
10:    end for
11:  end if
12: end for

```

---

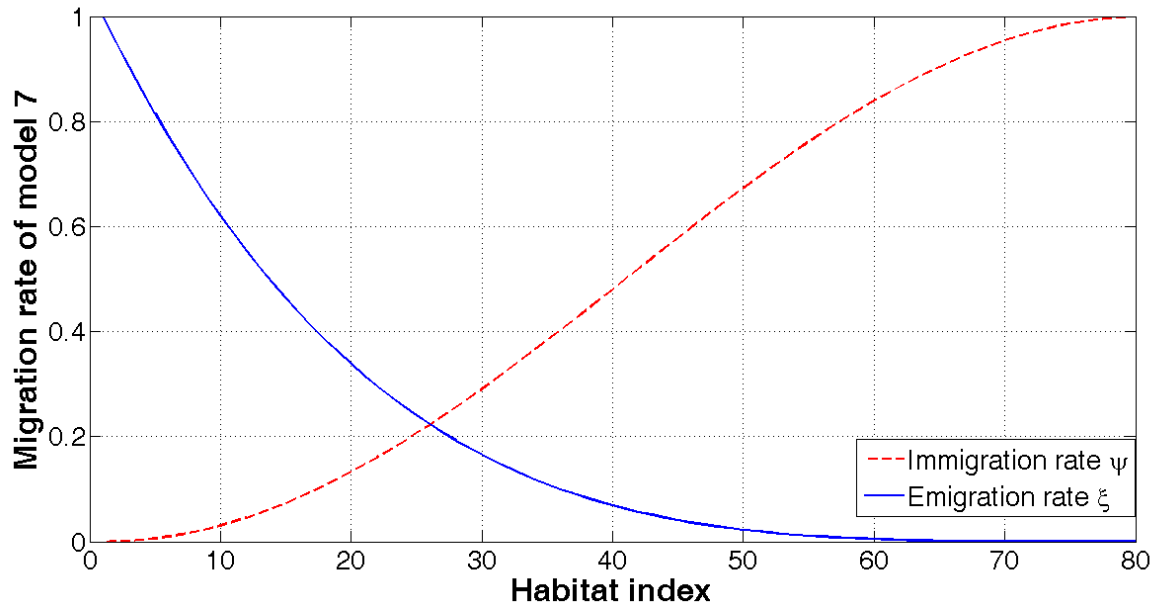


FIGURE 3 Migration Model 7:Habitat index vs migration rates for population size  $NP = 80$

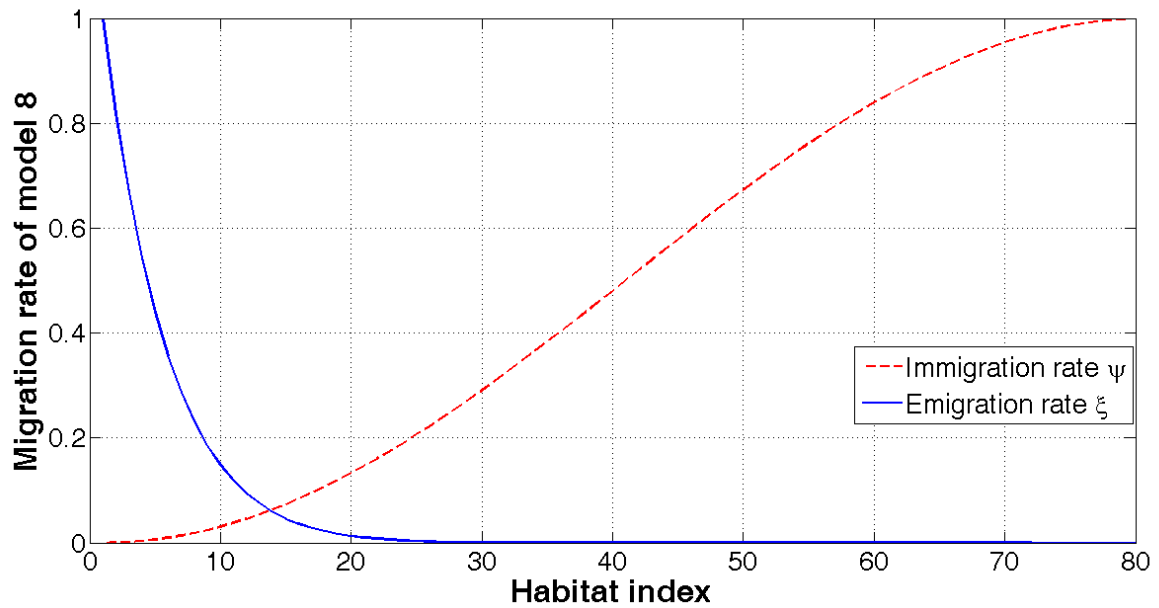


FIGURE 4 Migration Model 8:Habitat index vs migration rates for population size  $NP = 80$

The  $PMV_i$  and  $PMV_j$  in the algorithm 1 represent  $PMV_s$   $i$  and  $j$  respectively. In the BBO algorithm, the migration is not the only mechanism that is used in order to modify existing solutions i.e., habitats, but a mutation operator exists as well. A possible solution  $Q$  has a mutation rate  $m$ , which is a function of the solution probability, which is expressed as<sup>24</sup>:

$$m(Q) = m_{\max} \left( \frac{1 - P_q}{P_{\max}} \right) \quad (10)$$

where  $P_q$  is the probability a habitat contains  $Q$  species;  $P_{\max}$  is the maximum  $P_q$  value over all  $q \in [1, Q_{\max}]$ , and  $m_{\max}$  is a user-defined parameter. The goal of the mutation operator is to make the population more diverse. If there was not a mutation operator, then the algorithm would favor the most probable solutions to become predominant among the other vectors in the population, thus reducing diversity. With this mutation operator the low HSI (low fitness) solutions are more probable likely to mutate, thus they could be improved. Moreover, the good high HSI solutions also probable to mutate and to improve further. The mutation procedure can be described in Algorithm 2. Simon in<sup>24</sup> describes how  $P_q$  is varied from time  $t$  to time  $t + \Delta t$  as:

$$P_q(t + \Delta t) = P_q(t) (1 - \lambda_q \Delta t - \mu_q \Delta t) + P_{q-1}(t) \lambda_{q-1} \Delta t + P_{q+1}(t) \mu_{q+1} \Delta t \quad (11)$$

If consider the limit of  $\Delta t \rightarrow 0$  in 11 then we get the following expression<sup>24</sup>

$$\dot{P}_k = \begin{cases} -(\xi_0 + \psi_0) P_0 + \psi_1 P_1, & k = 0 \\ -(\xi_k + \psi_k) P_k + \psi_{k+1} P_{k+1} + \xi_{k-1} P_{k-1}, & 1 \leq k \leq Q_{\max} - 1 \\ -(\xi_{Q_{\max}} + \psi_{Q_{\max}}) P_{Q_{\max}} + \xi_{Q_{\max}-1} P_{Q_{\max}-1}, & k = Q_{\max} \end{cases} \quad (12)$$

---

#### Algorithm 2 *PMV* mutation

---

```

1: for  $n=1$  to  $NP$  do
2:   Calculate the probability  $P_n$ 
3:   Choose the  $SIV$   $PMV_k^n$  using probability that depends on  $P_n$ 
4:   if  $random(0, 1) < m_n$  then
5:     Generate randomly a  $SIV$  and then replace  $PMV_k^n$ 
6:   end if
7: end for

```

---

where  $PMV_k^n$  denotes the  $k$ -th  $SIV$  of the  $n$ -th  $PMV$ . The concept of elitism is also used in BBO. This requires the setting of an additional control parameter the number of elites, which is usually called  $p$ . In particular, in each generation we select the  $p$  best solutions and these survive to the next generation. The steps in the BBO antenna selection algorithm are summarized as follows:

- **Step 1:** Set the BBO control parameters. Set the maximum number of generations  $G_{\max}$ . Moreover, generate a random population from a uniform distribution that contains  $NP$  and  $PMV$  vectors.  $NP$  denotes the population size. Each  $PMV$  vector consists of  $K_R$ , it receive  $SIV$ s and it transmits  $K_T$   $SIV$ s. Thus, each  $PMV$  vector contains  $(K_R + K_T)$   $SIV$ s. As mentioned before, each  $SIV$  value follows the bit representation. At that time, the full matrix of  $NP \times (K_R + K_T)$  is generated.
- **Step 2:** Compute the cost function values for each  $PMV$  vector of the population, as stated by equation (3).
- **Step 3:** For each  $PMV$  vector of the population, map the capacity value to the number of species  $Q$ , the immigration rate  $\xi_k$  and the emigration rate  $\psi_k$ , from equations (6)-(9) depending on the migration model selected.
- **Step 4:** Employ migration only for non-elite habitats ( $PMV$  vectors) according to Algorithm 1.
- **Step 5:** Update the species count probability by applying<sup>24</sup>:
- **Step 6:** Apply equation (10) to mutate the no elite habitats.
- **Step 7:** Sort the population members according to the value of the cost function (capacity) in a descending order.
- **Step 8:** Replace the  $p$  worst  $PMV$  values with the previous generation elites.
- **Step 9:** Goto step 3 if current generation is less than  $G_{\max}$ .

Then select the  $PMV$  vector with the best cost function value. After that, the antennas corresponding to the  $L_R$  highest receive  $SIV$ s and the  $L_T$  highest transmit  $SIV$ s are chosen as the desired antenna subset. Figure 5 shows the flowchart of the BBO algorithm. More information about the BBO algorithm are found in<sup>40,24</sup>.

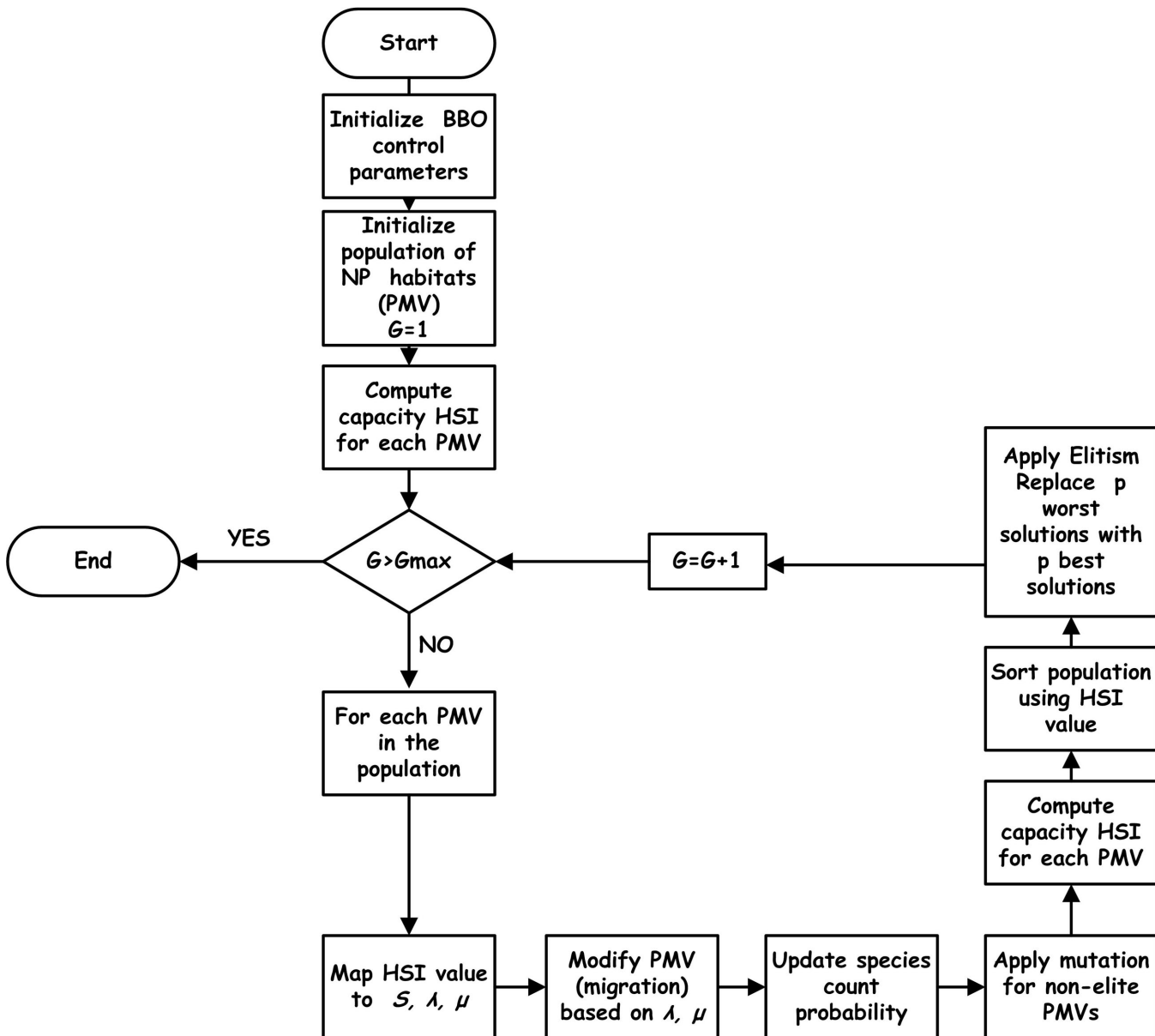


FIGURE 5 The BBO algorithm flowchart for the antenna selection problem.

## 5 | EVALUATION AND SIMULATION RESULTS

This section presents the evaluation set-up and the simulation results. We consider a  $16 \times 16$  MIMO system. We apply the original BBO, BBO7 and BBO8 to the channel capacity maximization problem. Moreover, we compare them with RVGA<sup>18</sup> and ACO. The fitness function selected is that given by (5). We assume four antenna selection scenarios,  $(L_T, L_R) = \{(2, 4), (3, 5), (4, 6), (8, 8)\}$  for five different  $SNR$  values.

In BBO algorithms, for both migration models we select the following values for the control parameters. We set  $P_{\text{mod}} = 1$ ,  $m_{\text{max}} = 0.005$ , and  $I = 1, E = 1$ . For the RVGA we adopt from<sup>18,19</sup> the values for the crossover probability  $pc = 0.5$  and the mutation probability  $pm = 0.09$ . For ACO we set, the initial pheromone value  $\tau_0 = 10^{-6}$ , the pheromone update constant  $Q = 20$ , the exploration constant  $q_0 = 1$ , the global pheromone decay rate  $\rho_g = 0.9$ , the local pheromone decay rate  $\rho_l = 0.5$ , the pheromone sensitivity  $\alpha = 1$  and the visibility sensitivity is  $\beta = 5$ . Moreover, for all the algorithms, we set the population size  $NP$ , the maximum number of generations  $G$ , and the elitism parameter  $p$  same as in<sup>18,19</sup>. These values are  $NP = 80, G =$

{12, 25, 40} for  $(L_T, L_R) = \{(2, 4), (3, 5), (4, 6)\}$ , respectively and  $p = 4$ . For the last scenario,  $(L_T, L_R) = (8, 8)$ , we select  $NP = 80$ ,  $G = 50$  and  $p = 4$ .

We run Monte-Carlo simulations using 10,000 channel realizations in total. In order to compare the algorithms performance, we calculate the mean/ergodic capacity and the outage capacity. Additionally, we will examine the dispersion of values of each algorithm presented graphically using box plots. The final comparison of the numerical results is based on non-parametric statistical tests.

**TABLE 1** Comparative results of Ergodic capacity with different  $SNR$  values for different  $(L_T, L_R)$  combinations. The larger values are denoted with bold font.

$(L_T, L_R) = (2, 4)$					
SNR (dB)	BBO7	BBO8	BBO	RVGA	ACO
0	5.121	<b>5.146</b>	5.035	5.051	4.824
5	8.052	<b>8.078</b>	7.938	7.969	7.656
10	11.218	<b>11.261</b>	11.128	11.154	10.501
15	14.501	<b>14.557</b>	14.412	14.449	14.209
20	17.827	<b>17.866</b>	17.714	17.749	17.285
$(L_T, L_R) = (3, 5)$					
SNR (dB)	BBO7	BBO8	BBO	RVGA	ACO
0	6.333	<b>6.355</b>	6.245	6.261	5.703
5	<b>10.494</b>	10.483	10.367	10.383	9.904
10	15.163	<b>15.165</b>	15.016	15.042	14.493
15	20.012	<b>20.049</b>	19.894	19.923	18.827
20	24.972	<b>24.996</b>	24.831	24.872	24.203
$(L_T, L_R) = (4, 6)$					
SNR (dB)	BBO7	BBO8	BBO	RVGA	ACO
0	<b>7.338</b>	7.319	7.244	7.283	6.611
5	<b>12.581</b>	12.555	12.456	12.479	11.454
10	<b>18.647</b>	18.638	18.525	18.547	17.029
15	25.102	<b>25.107</b>	24.956	25.009	24.084
20	31.668	<b>31.68</b>	31.528	31.575	30.073
$(L_T, L_R) = (8, 8)$					
SNR (dB)	BBO7	BBO8	BBO	RVGA	ACO
0	<b>9.097</b>	9.093	9.005	9.084	8.507
5	<b>16.991</b>	16.966	16.816	16.932	15.992
10	<b>27.401</b>	27.371	27.124	27.265	25.811
15	<b>39.424</b>	39.383	39.084	39.2	37.682
20	<b>52.168</b>	52.105	51.756	52.024	50.123

Tables 1 shows Ergodic capacity values obtained by all algorithms. Additionally, Table 2 summarizes the algorithms comparative results. More specifically Table 2 reports the number of times that each algorithm ranked first in terms of ergodic capacity

**TABLE 2** Comparative results of algorithms ranking first. Ergodic capacity with different  $SNR$  values for different  $(L_T, L_R)$  combinations.

SNR (dB)	BBO7	BBO8	BBO	RVGA	ACO
0	2	2	0	0	0
5	3	1	0	0	0
10	2	2	0	0	0
15	1	3	0	0	0
20	1	3	0	0	0

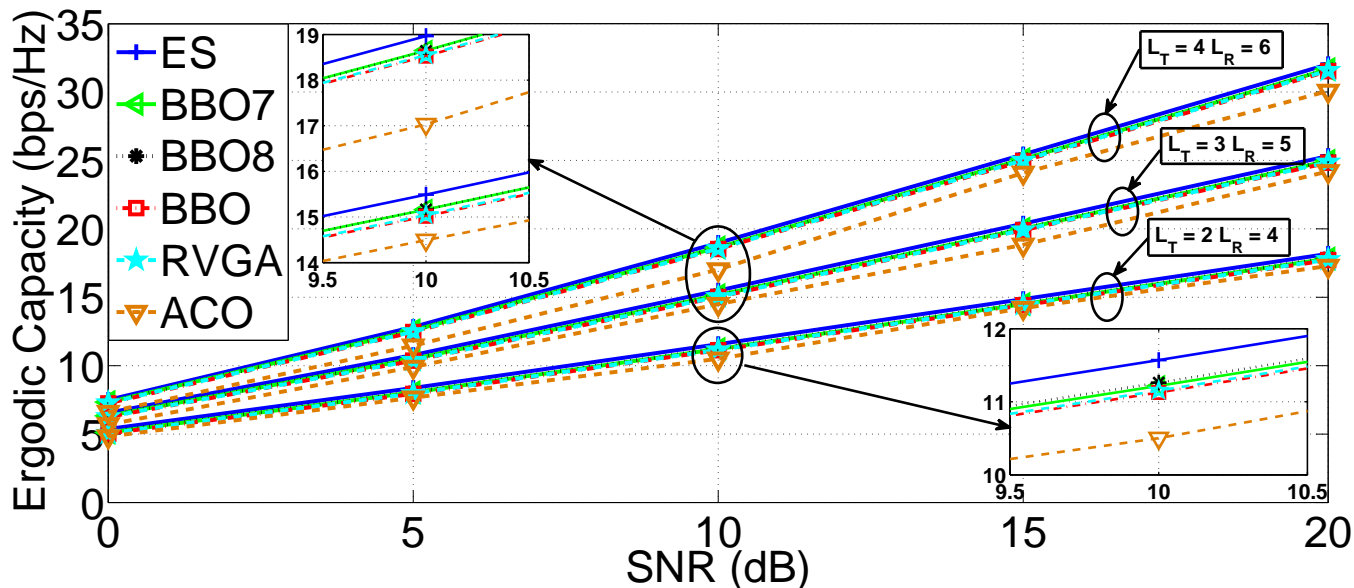


**FIGURE 6** Ergodic capacity versus  $SNR$  for different  $(L_T, L_R)$  combinations. The insets show graph details.

values. The obtained results are for five different  $SNR$  values starting from 0 dB to 20 dB with step 5 dB, and four different transmit-receive antenna scenarios. It can be clearly seen from Tables 1 that, BBO8 and BBO7 perform better among the other evolutionary algorithms. We notice that BBO8 exceeds the performance of the other algorithms in 11 out of the 20 cases, while BBO7 achieves the best value in 9 out of the 20 cases. More specifically, BBO8 is superior to the other algorithms for the first two cases:  $(L_T, L_R) = (2, 4)$  and  $(L_T, L_R) = (3, 5)$ , while BBO7 is slightly inferior. In the other two scenarios  $(L_T, L_R) = (4, 6)$  and  $(L_T, L_R) = (8, 8)$ , BBO7 obtains the solution with the highest capacity value, while BBO8 is second best. For the remaining algorithms, we should mention that RVGA competes the original BBO with the linear model in each scenario, resulting in slightly better performance. Moreover, ACO is inferior for this problem. In Figures 6 and 7, the ergodic capacity is plotted versus the  $SNR$  for all algorithms. We notice from Figure 6 that BBO8 and BBO7 results are close. For most of the cases BBO8 is better, while the RVGA results are close to these of the two BBO non-linear models and almost overlaps with the others. The BBO8 and BBO7 results are slightly inferior to the ES. Moreover from Figure 7 and Table 1, it is obvious that BBO7 outperforms the other algorithms. In both figures the ES obtains always the best results.

Figures 8-11 show the complimentary cumulative distribution functions (CCDFs) for the four different cases:  $(L_T, L_R) = \{(2, 4), (3, 5), (4, 6), (8, 8)\}$  with  $SNR = 10dB$ . In all Figures the ES presents the best results. BBO8 and BBO7 are close to that performance. From Figure 8 we notice that BBO8 and BBO7 clearly are superior to the RVGA and the original BBO. The RVGA and the original BBO results are very close. The same picture is also the case in Figure 9 where BBO8 and BBO7 outperform the other algorithms. Moreover, it is evident from Figure 10 that the non-linear models obtain performance very close to that of the ES. The original BBO and the RVGA plots almost overlap. Additionally, Figure 11 shows that RVGA and the original BBO are slightly inferior to the BBO7 and BBO8. Overall, it is obvious that, BBO8 and BBO7 performance is superior to the

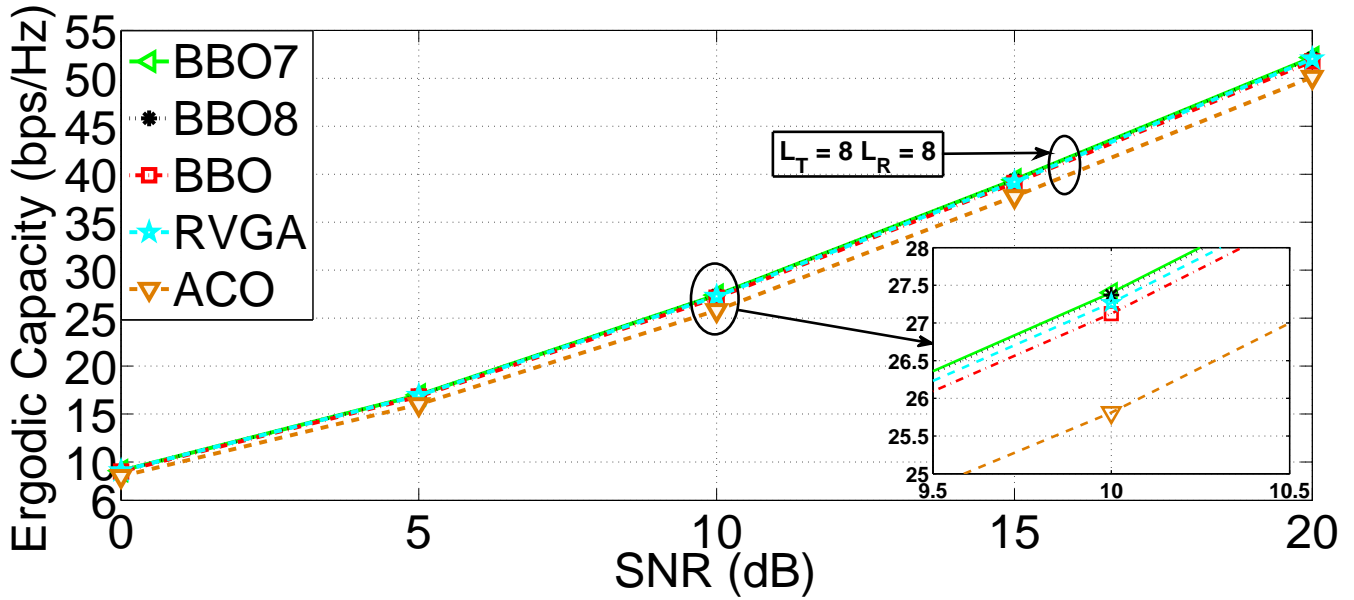


FIGURE 7 Ergodic capacity versus  $SNR$  for  $(L_T, L_R) = (8, 8)$ . The insets show graph details.

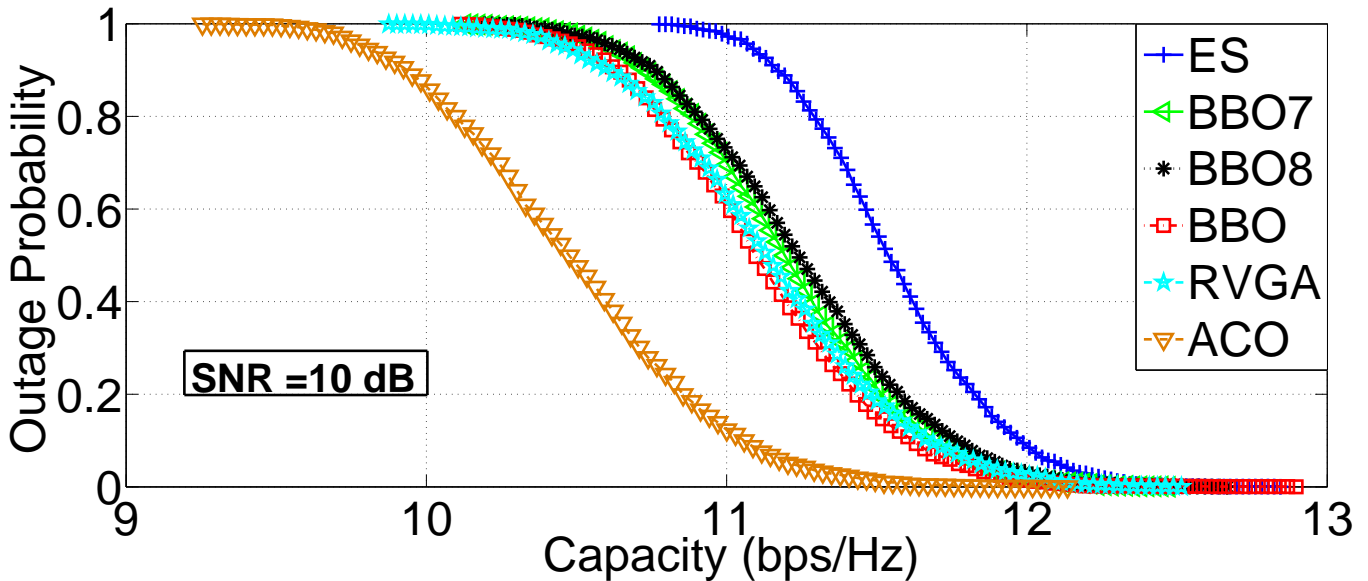


FIGURE 8 CDFs of capacities for  $(L_T, L_R) = (2, 4)$  at  $SNR = 10dB$ .

other algorithms. In the first two cases, BBO8 retains its first place in terms of maximum capacity value, while BBO7 is the best algorithm according to the more complex cases, i.e.,  $(L_T, L_R) = \{(4, 6), (8, 8)\}$ . Moreover, the other EAs performance is similar to that of Figure 8. The ACO performance is the worst among the other algorithms in all cases.

Table 3 reports the 1% probability of capacity outage results. Moreover, Table 4 reports the comparative results of algorithms ranking first for the 1% outage capacity case. In this case, BBO7 obtains the best results in most of the cases (17 out of 20), while BBO model 8 performs better in 3 out of the 20 cases. The 1% outage capacity results are also presented graphically in Figures 12 and 13 (for an  $SNR$  range of 0 to 20 dB). We can notice that the outage capacity found using the BBO7 is closer to the outage capacity offered by the ES regardless of the scenario that is being used. BBO8 is slightly inferior to BBO7, while

**TABLE 3** Comparative results of 1% Outage capacity with different  $SNR$  values for different  $(L_T, L_R)$  combinations. The larger values are denoted with bold font.

$(L_T, L_R) = (2, 4)$					
SNR (dB)	BBO7	BBO8	BBO	RVGA	ACO
0	<b>4.43</b>	<b>4.43</b>	4.367	4.319	4.095
5	<b>7.255</b>	7.212	7.106	7.103	6.616
10	<b>10.391</b>	10.369	10.26	10.19	9.599
15	<b>13.647</b>	13.615	13.6	13.501	13.463
20	16.965	<b>17.02</b>	16.858	16.803	16.583
$(L_T, L_R) = (3, 5)$					
SNR (dB)	BBO7	BBO8	BBO	RVGA	ACO
0	5.514	<b>5.557</b>	5.426	5.401	5.098
5	<b>9.528</b>	9.412	9.33	9.385	9.1
10	<b>14.096</b>	14.061	13.893	13.923	13.481
15	<b>18.906</b>	18.876	18.737	18.668	17.74
20	<b>23.885</b>	23.837	23.712	23.682	23.233
$(L_T, L_R) = (4, 6)$					
SNR (dB)	BBO7	BBO8	BBO	RVGA	ACO
0	<b>6.453</b>	6.383	6.365	6.357	5.606
5	11.414	<b>11.433</b>	11.293	11.2	10.086
10	<b>17.378</b>	17.2	17.273	17.206	15.693
15	<b>23.815</b>	23.714	23.671	23.6	22.906
20	<b>30.292</b>	30.263	30.146	30.128	28.699
$(L_T, L_R) = (8, 8)$					
SNR (dB)	BBO7	BBO8	BBO	RVGA	ACO
0	<b>8.116</b>	8.079	7.985	8.082	7.534
5	<b>15.563</b>	15.529	15.435	15.443	14.642
10	<b>25.421</b>	25.368	25.04	25.313	24.08
15	<b>37.245</b>	37.128	36.853	36.853	35.79
20	<b>49.95</b>	49.75	49.561	49.477	48.075

**TABLE 4** Comparative results of algorithms ranking first. 1% Outage capacity with different  $SNR$  values for different  $(L_T, L_R)$  combinations.

SNR (dB)	BBO7	BBO8	BBO	RVGA	ACO
0	3	1	0	0	0
5	3	1	0	0	0
10	4	0	0	0	0
15	4	0	0	0	0
20	3	1	0	0	0

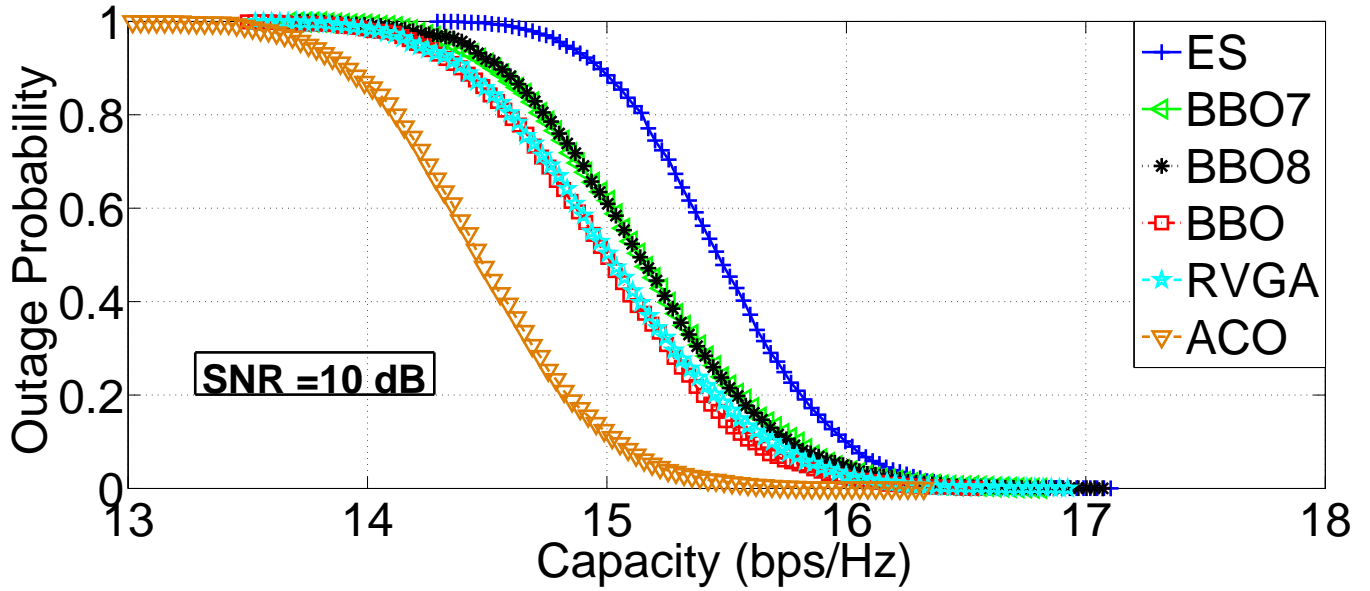


FIGURE 9 CDFs of capacities for  $(L_T, L_R) = (3, 5)$  at  $SNR = 10dB$ .

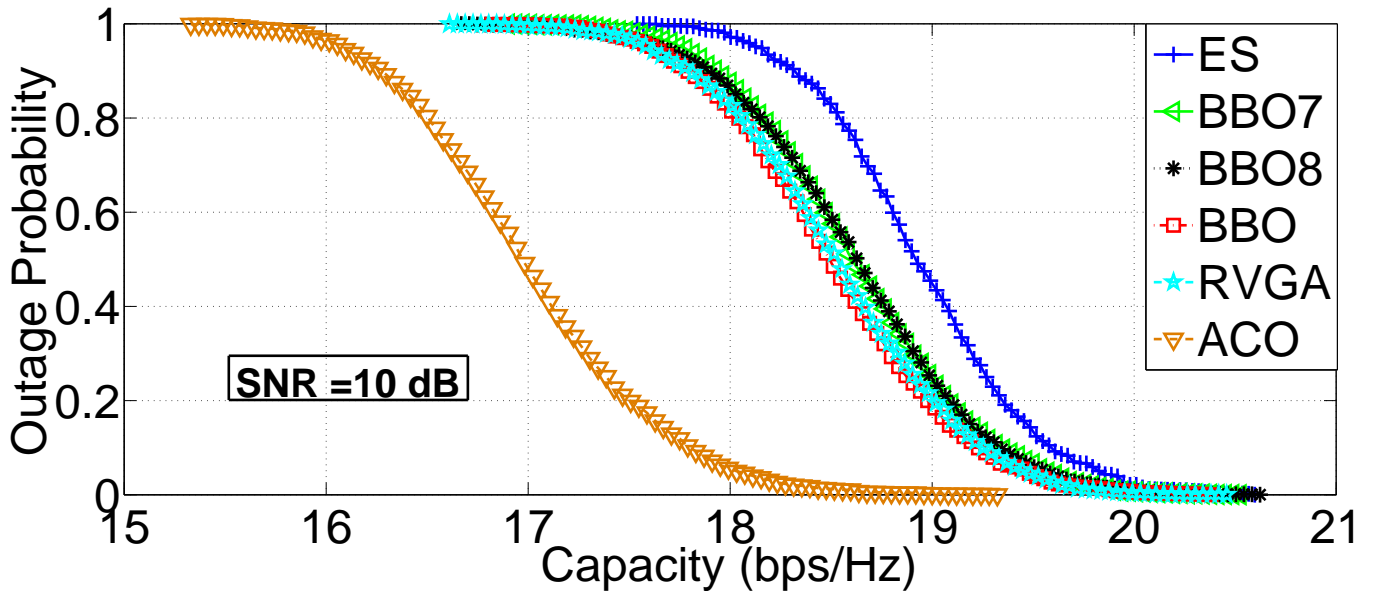


FIGURE 10 CDFs of capacities for  $(L_T, L_R) = (4, 6)$  at  $SNR = 10dB$ .

BBO linear model is in the third place performing slightly better than the RVGA. Additionally, from Figures 12 and 13 it is obvious that ACO obtains the worst performance.

Figs 14-17 depict the dispersion using box plots for each algorithm at  $SNR = 10dB$ . All the algorithms have similar value spread in each scenario, with the BBO7 and BBO8 achieving a higher median value. BBO7 shows a slightly smaller dispersion of values compared to BBO8. The original BBO and the RVGA seem to obtain similar median capacity values. It is interesting to note that the value of the spread seems to be independent of the number of antennas and shows the performance differences between the algorithms.

It is worth mentioning that in all cases the BBO algorithm with the non-linear models obtains the best results. A possible explanation of this is attached to the unique BBO features. In particular, BBO has a unique way for sharing information

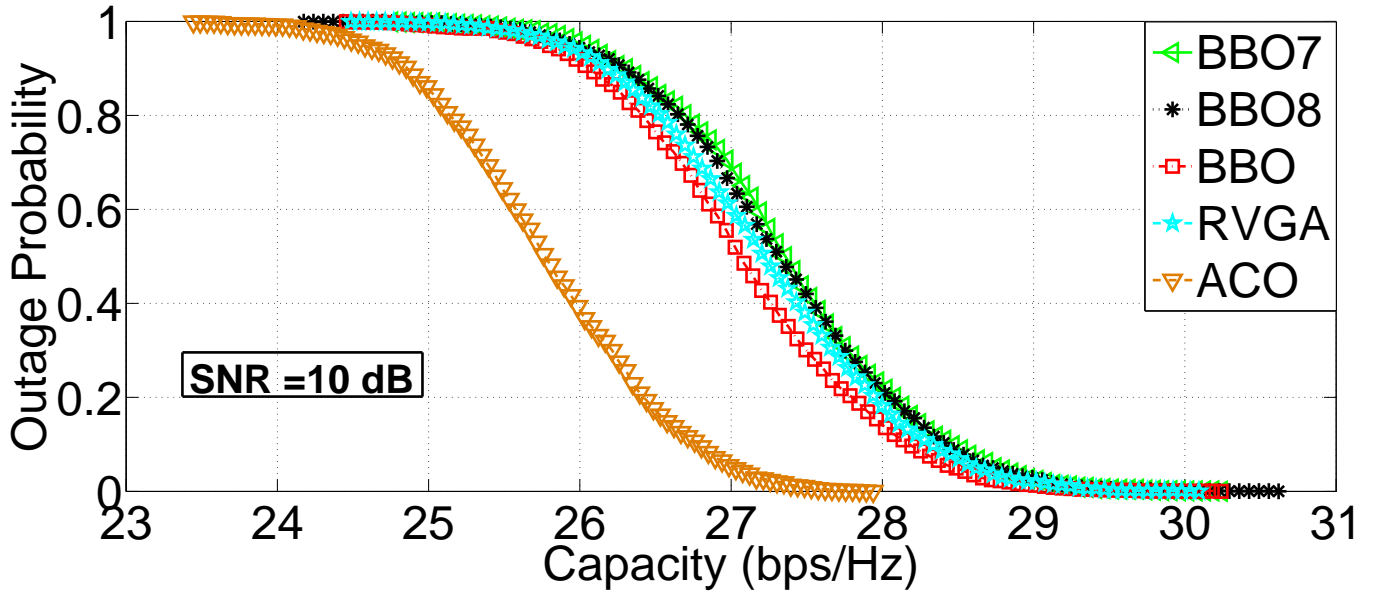


FIGURE 11 CDFs of capacities for  $(L_T, L_R) = (8, 8)$  at  $SNR = 10dB$ .

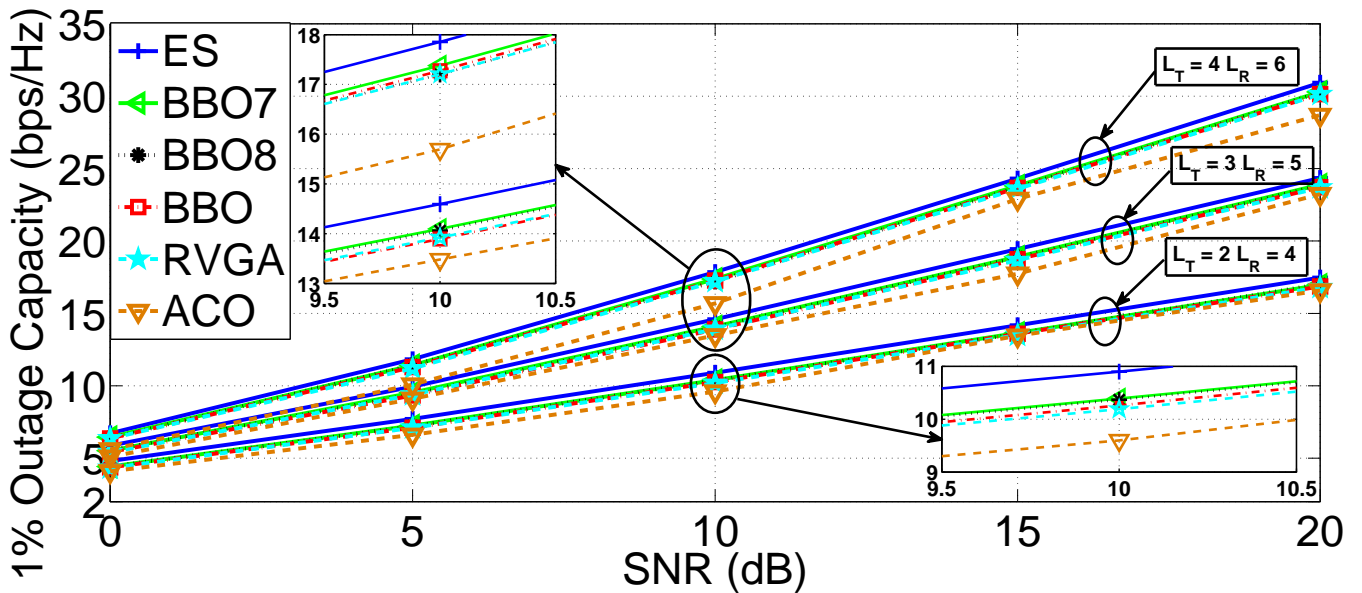


FIGURE 12 1% Outage capacity versus  $SNR$  for different  $(L_T, L_R)$  combinations. The insets show graph details.

among different individuals that does not exist in other algorithms like RVGA and ACO. For example, contrary to the RVGA and ACO, BBO uses the migration model in order to change and improve the population from one generation to the next, where the  $HSI$  value of each vector determines the emigration and the immigration rates. Thus, in BBO the sharing mechanism among the population vectors is the migration models. This sharing mechanism through migration helps BBO to have a good exploitation ability. Moreover, it seems that the use of the non-linear models with high  $K$  value results in better performance than the original BBO, as it reported in<sup>25</sup>. Additionally, BBO works in the discrete space, if the original values are in discrete space, while RVGA works in real space. Both migration models have the same immigration rate equation, while their emigration rate equations are similar. Thus, this could explain the fact that both models results are close.

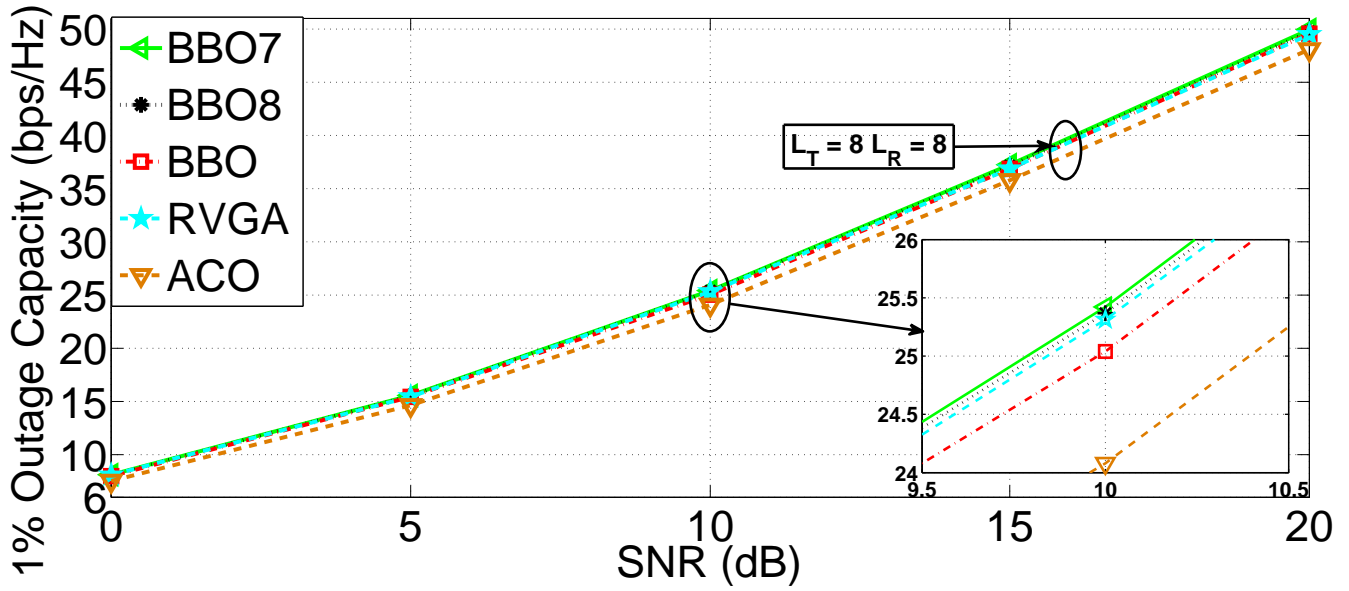


FIGURE 13 1% Outage capacity versus  $SNR$  for  $(L_T, L_R) = (8, 8)$ . The insets show graph details.

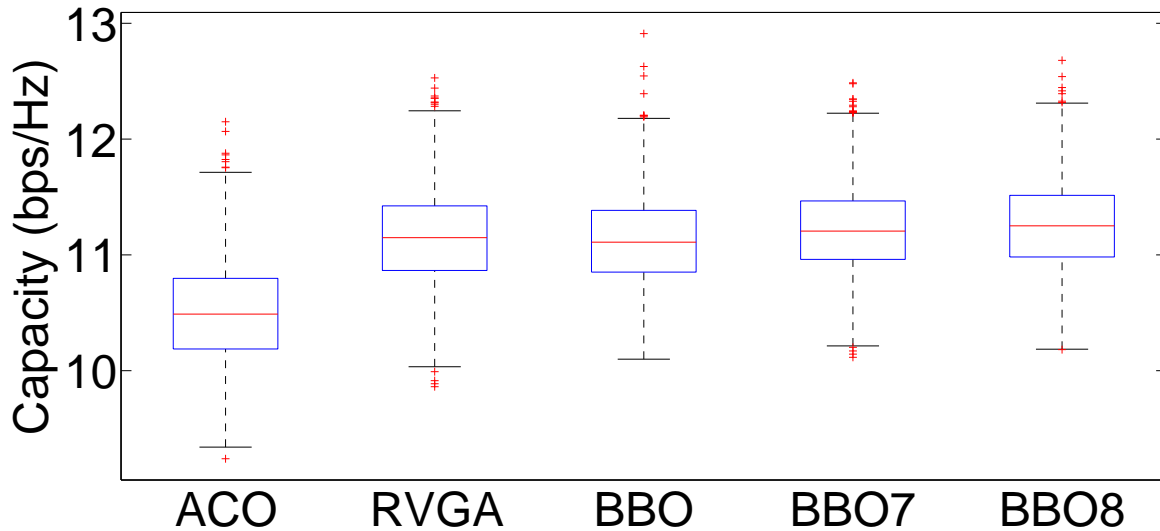


FIGURE 14 Box plots of capacity values distribution for each algorithm for  $(L_T, L_R) = (2, 4)$  at  $SNR = 10dB$ .

### 5.1 | Non-parametric statistical tests

Additionally, in order to compare the algorithms performance we have conducted non-parametric statistical tests. These are the Friedman test and the Wilcoxon signed-rank test, which have been used as a metric for the performance evaluation of EAs<sup>41,42,43</sup>. We perform these tests using data from the results reported in Tables 2 and 4. Tables 5 and 6 hold the ranking results for both tests. It is obvious that BBO7 algorithm ranked first and outperforms the other algorithms.

In order to examine if BBO7 actually outperforms the other methods, we set the significant level for the Wilcoxon signed-rank test to 0.05. In Table 6, all the  $p$ -values found (shown in bold font) are below the significance level (0.05) for the case of BBO7 vs. the other methods. Therefore, the null hypothesis can be rejected and we can accept that a significant difference exists

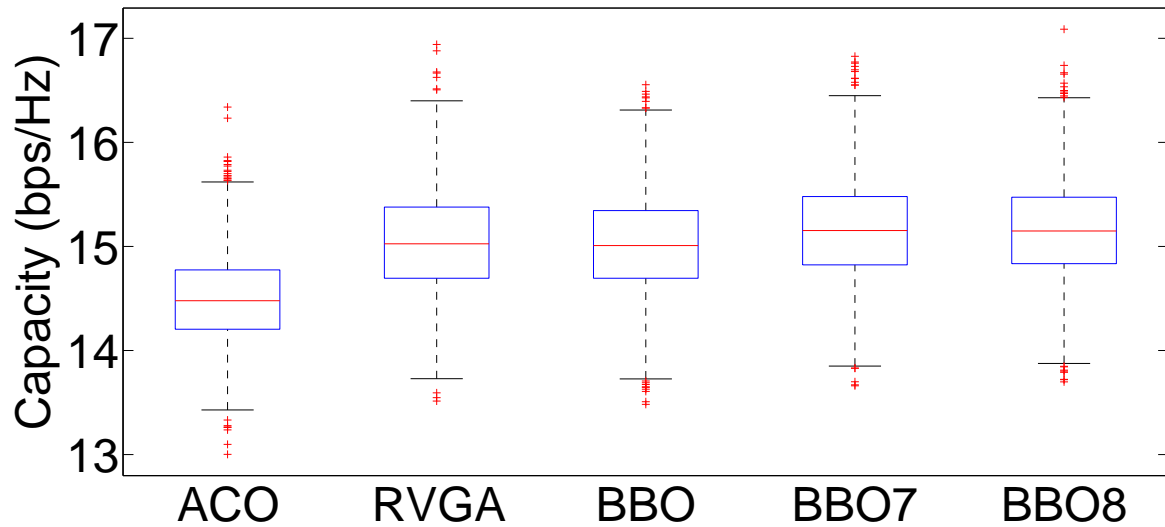


FIGURE 15 Box plots of capacity values distribution for each algorithm for  $(L_T, L_R) = (3, 5)$  at  $SNR = 10dB$ .

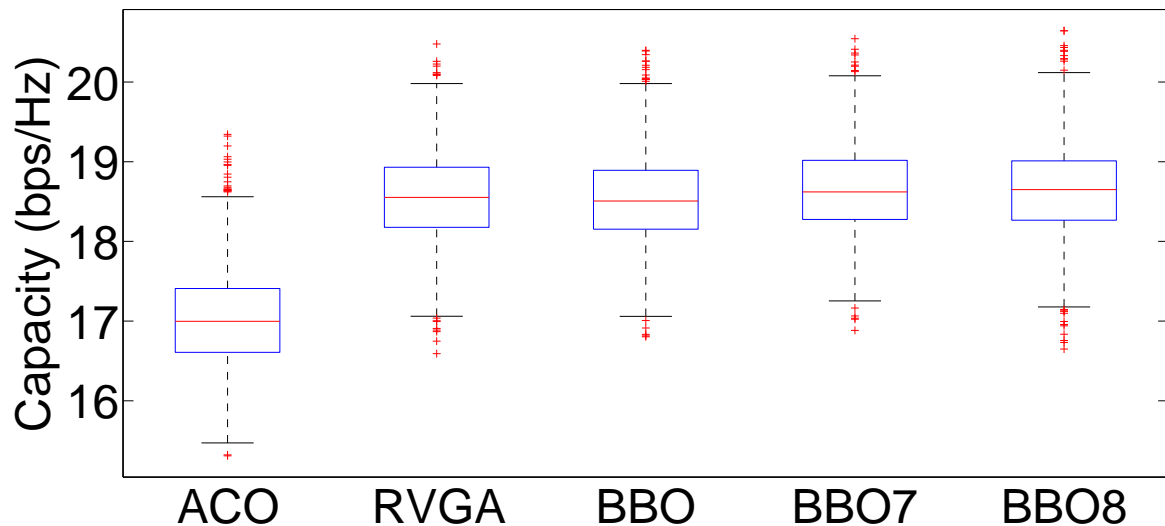


FIGURE 16 Box plots of capacity values distribution for each algorithm for  $(L_T, L_R) = (4, 6)$  at  $SNR = 10dB$ .

between BBO7 and the other methods. Thus, BBO7 is proven to be significantly better than BBO8, the original BBO algorithm, RVGA and ACO.

## 5.2 | Complexity of the BBO-AS algorithm

It is also useful to comment on the complexity of the algorithms that affects implementation. We have used similar implementations for all algorithms as in<sup>24</sup>, thus every algorithm uses elitism and sorts population from best to worst at the end of

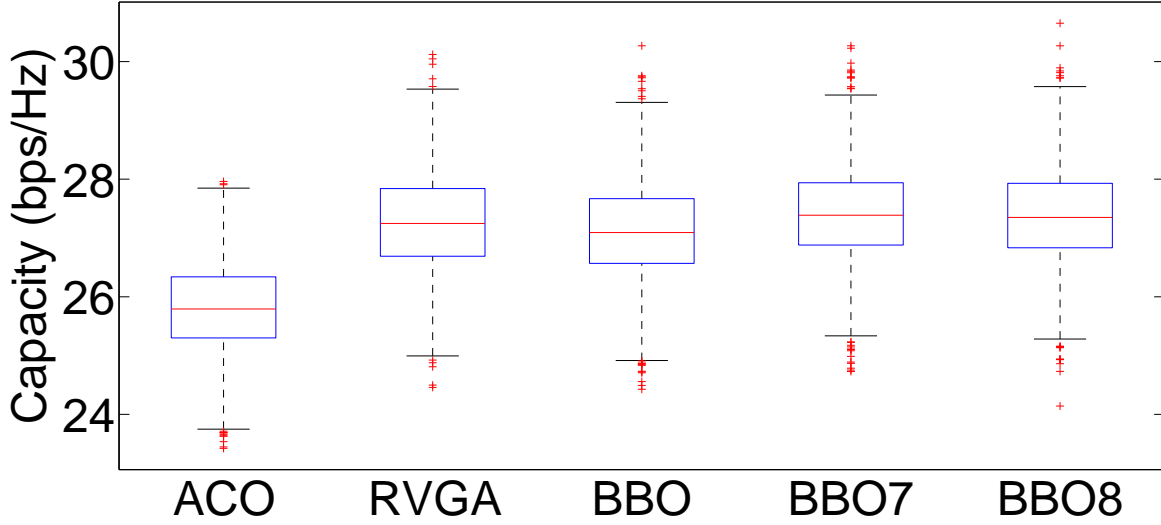


FIGURE 17 Box plots of capacity values distribution for each algorithm for  $(L_T, L_R) = (8, 8)$  at  $SNR = 10dB$ .

TABLE 5 Average Rankings achieved by Friedman test.

Method	Average Rank	Normalized values	Rank
<b>BBO7</b>	<b>1.35</b>	<b>1</b>	<b>1</b>
<b>BBO8</b>	1.71	1.27	2
<b>BBO</b>	3.6	2.67	4
<b>RVGA</b>	3.34	2.47	3
<b>ACO</b>	5	3.7	5

TABLE 6 Wilcoxon signed-rank test between BBO7 and the other algorithms. The bold font indicates values below significant level.

BBO7 vs	p-values
BBO8	<b>0.0346</b>
BBO	<b>2.05E-08</b>
RVGA	<b>2.51E-08</b>
ACO	<b>1.16E-08</b>

each iteration. Therefore, the time complexity of all used algorithms is the same. The BBO time complexity at each iteration is  $\mathcal{O}(NP^2K + NPg)$ , where  $g$  is the time complexity of the cost function, and  $K$  is the problem dimension. The time complexity of each objective function evaluation is  $\mathcal{O}(L_R L_T^2)$ <sup>18</sup>, which contains a matrix multiplication of an  $L_T \times L_R$  matrix with an  $L_R \times L_T$  matrix. Therefore, the overall complexity of the BBO algorithm in the AS problem at each iteration is  $\mathcal{O}(NP^2(K_R + K_T) + NPL_R L_T^2)$ . The computational complexity for the ES is far greater than the one produced by the BBO, since it examines all the possible antenna subset combinations. Namely, we have  $2184 \times 10^2$ ,  $2446 \times 10^3$ ,  $1457 \times 10^4$  and  $1656 \times 10^5$  different antenna subset combinations for each scenario:  $(L_T, L_R) = \{(2, 4), (3, 5), (4, 6), (8, 8)\}$  respectively. On the other hand, the number of objective-function evaluations for each algorithm is the same, given by the product  $NP \times G$ . This translates to 960, 2000, 3200 and 4000 antenna subsets for each scenario:  $(L_T, L_R) = \{(2, 4), (3, 5), (4, 6), (8, 8)\}$  respectively,

in order to execute the capacity calculations. Bearing that in mind, ES is a time consuming method with increased computational complexity, which is impractical for complex problems. The BBO algorithm could be hardware implemented for real-time applications as it is reported in<sup>44</sup>.

## 6 | CONCLUSION

In this paper, we proposed the application of the BBO algorithm in the problem of joint transmit/receive antenna selection in MIMO wireless systems. We have evaluated the original BBO algorithm performance as well as its different migration models with other evolutionary algorithms using the capacity maximization criterion. The simulation results showed that, in terms of ergodic capacity, and for low computational complexity scenarios, i.e.,  $(L_T, L_R) = (2, 4), (3, 5)$ , the BBO antenna selection algorithm that uses the migration model 7 outperformed the other EAs, while BBO8 obtained the second best results. Additionally, for higher computational complexity scenarios, i.e.,  $(L_T, L_R) = (4, 6), (8, 8)$ , BBO7 obtained results with the highest ergodic capacity value. Furthermore, with regard to 1% outage capacity, BBO7 was much closer to the ES methods results of several combinations (LT, LR) of transmit and receive antennas and outperformed BBO8 in all scenarios. Both non-linear migration models outperformed the original BBO linear model. In accordance with the previous analysis, it is evident that, with its overall performance, BBO migration model 7 fulfils the AS criterion for the maximization of the MIMO channel capacity, especially for high computational complexity cases of operating antennas in the transceiver. In our future work, we will examine massive MIMO scenarios and evaluate how the performance of BBO migration models is scaled.

## ACKNOWLEDGMENTS

The work of C.Kalialakis was supported under EU H2020 Marie Skłodowska-Curie Grant Agreement 654734.

## Conflict of interest

The authors declare no potential conflict of interests.

## References

1. Goldsmith A., Paulraj A., Calderbank R., Poor H. V., Biglieri E., Constantinides A.. *An Introduction to MIMO Communication*. Cambridge University Press; 2006.
2. Molisch A. F., Win M. Z.. Mimo systems with antenna selection. *IEEE Microwave Magazine*. 2004;5(1):46–56.
3. Telatar E.. Capacity of multi-antenna Gaussian channels. *European Transactions on Telecommunications*. 1999;10(6):585–595.
4. Molisch A. F., Win M. Z., Choi Y. S., Winters J. H.. Capacity of MIMO systems with antenna selection. *IEEE Transactions on Wireless Communications*. 2005;4(4):1759–1771.
5. Amadori P. V., Masouros C.. Interference-Driven Antenna Selection for Massive Multiuser MIMO. *IEEE Transactions on Vehicular Technology*. 2016;65(8):5944–5958.
6. Benmimoune M., Driouch E., Ajib W., Massicotte D.. Feedback reduction and efficient antenna selection for massive MIMO system. In: Institute of Electrical and Electronics Engineers Inc.; 2015.
7. Benmimoune M., Driouch E., Ajib W., Massicotte D.. Novel transmit antenna selection strategy for massive MIMO downlink channel. *Wireless Networks*. 2016;:1–12.
8. Gao X., Edfors O., Tufvesson F., Larsson E. G.. Multi-switch for antenna selection in massive MIMO. In: Institute of Electrical and Electronics Engineers Inc.; 2015.

9. Chen C. E.. A computationally efficient near-optimal algorithm for capacity- maximization based joint transmit and receive antenna selection. *IEEE Communications Letters*. 2010;14(5):402–404.
10. Chun N., Zhifeng T., Mehta N. B., et al. Antenna selection for next generation IEEE 802.16 mobile stations. *Proceedings of the IEEE International Conference on Communications*. 2008;.
11. Gore D. A., Paulraj A. J.. MIMO antenna subset selection with space-time coding. *IEEE Transactions on Signal Processing*. 2002;50(10):2580–2588.
12. Gorokhov A., Gore D. A., Paulraj A. J.. Receive antenna selection for MIMO spatial multiplexing: Theory and algorithms. *IEEE Transactions on Signal Processing*. 2003;51(11):2796–2807.
13. Sanayei S., Nosratinia A.. Antenna selection in MIMO systems. *IEEE Communications Magazine*. 2004;42(10):68–73.
14. Sanayei S., Nosratinia A.. Capacity of MIMO channels with antenna selection. *IEEE Transactions on Information Theory*. 2007;53(11):4356–4362.
15. Uchida D., Arai H., Inoue Y., Cho K.. Antenna selection based on minimum Eigenvalue in dual-polarized directional MIMO antenna. *Proceedings of the IEEE Vehicular Technology Conference (VTC 2010-Spring) IEEE*. 2010;71:15.
16. Phan K. T., Tellambura C.. Receive antenna selection based on union-bound minimization using convex optimization. *IEEE Signal Processing Letters*. 2007;14(9):609–612.
17. Karamalis P. D., Skentos N. D., Kanatas A. G.. Selecting array configurations for MIMO systems: An evolutionary computation approach. *IEEE Transactions on Wireless Communications*. 2004;3(6):1994–1998.
18. Lain J. K.. Joint transmit/receive antenna selection for MIMO systems: A real-valued genetic approach. *IEEE Communications Letters*. 2011;15(1):58–60.
19. Lu H. Y., Fang W. H.. Joint transmit/receive antenna selection in MIMO systems based on the priority-based genetic algorithm. *IEEE Antennas and Wireless Propagation Letters*. 2007;6:588–591.
20. Lu H. Y., Fang W. H.. Joint receive antenna selection and symbol detection for MIMO systems: A heterogeneous genetic approach. *IEEE Communications Letters*. 2009;13(2):97–99.
21. Naeem M., Lee D. C.. Low-complexity joint transmit and receive antenna selection for MIMO systems. *Engineering Applications of Artificial Intelligence*. 2011;24(6):1046–1051.
22. Naeem M., Lee D. C.. A joint antenna and user selection scheme for multiuser MIMO system. *Applied Soft Computing Journal*. 2014;23:366–374.
23. Tohidi M. S., Azmi P.. Low-complexity throughput-based antenna selection method. *Wireless Personal Communications*. 2014;75(1):385–395.
24. Simon D.. Biogeography-Based Optimization. *IEEE Transactions on Evolutionary Computation*. 2008;12(6):702–713.
25. Guo W., Wang L., Wu Q.. An analysis of the migration rates for biogeography-based optimization. *Information Sciences*. 2014;254:111–140.
26. Singh U., Kumar H., Kamal T. S.. Design of Yagi-Uda Antenna Using Biogeography Based Optimization. *IEEE Transactions on Antennas and Propagation*. 2010;58(10):3375–3379.
27. Lohokare M. R., Pattnaik S. S., Devi S., Panigrahi B. K., Bakwad K. M., Joshi J. G.. Modified BBO and calculation of resonant frequency of circular microstrip antenna. In: :487–492; 2009.
28. Lohokare M. R., Pattnaik S. S., Devi S., Bakwad K. M., Joshi J. G.. Parameter calculation of rectangular microstrip antenna using Biogeography-Based Optimization. In: :1–4; 2009.

29. Goudos S. K., Baltzis K. B., Siakavara K., Samaras T., Vafiadis E., Sahalos J. N.. Reducing the number of elements in linear arrays using biogeography-based optimization. In: 6<sup>th</sup> European Conference on Antennas and Propagation, EuCAP 2012:1615–1618; 2012.
30. Goudos S. K., Sahalos J. N.. Design of Large Thinned Arrays Using Different Biogeography-Based Optimization Migration Models. *International Journal of Antennas and Propagation*. 2016;2016.
31. Sharaq A., Dib N.. Design of linear and circular antenna arrays using biogeography based optimization. In: :1–6; 2011.
32. Singh U., Kumar H., Kamal T. S.. Linear array synthesis using biogeography based optimization. *Progress In Electromagnetics Research M*. 2010;11:25–36.
33. Fountoukidis K. C., Siakavara K., Goudos S. K., Kalialakis C.. Antenna selection for MIMO systems using biogeography based optimization. In: :319–322; 2017.
34. Dorigo M., Maniezzo V., Colorni A.. Ant system: Optimization by a colony of cooperating agents. *IEEE Transactions on Systems, Man, and Cybernetics, Part B: Cybernetics*. 1996;26(1):29–41.
35. Dorigo M., Stutzle T.. *Ant Colony Optimization*. Cambridge, MA: The MIT Press; 2004.
36. Quevedo-Teruel O., Rajo-Iglesias E.. Ant Colony Optimization in Thinned Array Synthesis With Minimum Sidelobe Level. *IEEE Antennas and Wireless Propagation Letters*. 2006;5(1):349–352.
37. Rajo-Iglesias E., Quevedo-Teruel Ó. Linear array synthesis using an ant-colony-optimization-based algorithm. *IEEE Antennas and Propagation Magazine*. 2007;49(2):70–79.
38. Wang Y., Dong Y.. A genetic antenna selection algorithm for massive MIMO systems with channel estimation error. In: :1–4; 2015.
39. Ma Haiping. An analysis of the equilibrium of migration models for biogeography-based optimization. *Information Sciences*. 2010;180(18):3444 - 3464.
40. Ma H., Simon D., Fei M., Chen Z.. On the equivalences and differences of evolutionary algorithms. *Engineering Applications of Artificial Intelligence*. 2013;26(10):2397–2407.
41. Derrac J., Garcia S., Molina D., Herrera F.. A practical tutorial on the use of nonparametric statistical tests as a methodology for comparing evolutionary and swarm intelligence algorithms. *Swarm and Evolutionary Computation*. 2011;1(1):3–18.
42. García S., Fernández A., Luengo J., Herrera F.. Advanced nonparametric tests for multiple comparisons in the design of experiments in computational intelligence and data mining: Experimental analysis of power. *Information Sciences*. 2010;180(10):2044–2064.
43. García S., Molina D., Lozano M., Herrera F.. A study on the use of non-parametric tests for analyzing the evolutionary algorithms' behaviour: A case study on the CEC'2005 Special Session on Real Parameter Optimization. *Journal of Heuristics*. 2009;15(6):617–644.
44. Kavitha R., Thottungal R.. FPGA based hardware implementation of WTHD minimisation in asymmetric multilevel inverter using biogeographical based optimisation. *Istanbul University - Journal of Electrical and Electronics Engineering*. 2015;14(2):1799–1807.
45. Baek M.-S., Kook H.-J., Kim M.-J., You Y.-H., Song H.-K.. Multi-antenna scheme for high capacity transmission in the digital audio broadcasting. *IEEE Transactions on Broadcasting*. 2005;51(4):551–559.
46. Dorigo M., Maniezzo V., Colorni A.. Ant system: Optimization by a colony of cooperating agents. *IEEE Transactions on Systems, Man, and Cybernetics, Part B: Cybernetics*. 1996;26(1):29–41.
47. Dritsoula L., Wang Z., Sadjadpour H. R., Garcia-Luna-Aceves J. J.. Antenna selection for opportunistic interference management in MIMO broadcast channels. In: :1–5; 2010.

48. Gharavi-Alkhansari M., Gershman A. B.. Fast antenna subset selection in MIMO systems. *IEEE Transactions on Signal Processing*. 2004;52(2):339–347.
49. Gómez-Calero C., Navarrete L.C., De Haro L., Martínez R.. A  $2 \times 2$  MIMO DVB-T2 System: Design, new channel estimation scheme and measurements with polarization diversity. *IEEE Transactions on Broadcasting*. 2010;56(2):184–192.
50. Hamdi K., Zhang W., Letaief K. B.. Low-Complexity Antenna Selection and user Scheduling in Cognitive MIMO Broadcast Systems. In: :4038–4042; 2008.
51. Khan M. A., Vesilo R., Davis L. M., Collings I. B.. User and Transmit Antenna Selection for MIMO Broadcast Wireless Channels with Linear Receivers. In: :276–281; 2008.
52. Lari M., Mohammadi A., Abdipour A., Lee I.. Characterization of effective capacity in antenna selection MIMO systems. *Journal of Communications and Networks*. 2013;15(5):476–485.
53. Park J., Lee S.. MIMO beamforming for QoS enhancement via analog, digital and hybrid relaying. *IEEE Transactions on Broadcasting*. 2010;56(4):494-503.
54. Xu J., Lee S.-J., Kang W.-S., Seo J.-S.. Adaptive resource allocation for mimo-ofdm based wireless multicast systems. *IEEE Transactions on Broadcasting*. 2010;56(1):98–102.
55. Zhang R., Ho C. K.. MIMO Broadcasting for Simultaneous Wireless Information and Power Transfer. *IEEE Transactions on Wireless Communications*. 2013;12(5):1989–2001.

